Journal of Textiles and Polymers

Vol. 12, No. 3, 3-10, July 2024
https://www.itast.ir
DOI: https://doi.org/10.48302/jtp.2025.526555.1314

Antibacterial properties of PCL-based nanofibers loaded with ZnO nanoparticles synthesized via sol-gel method

Sanam Amiri[1], S. Hajir Bahrami[1*] , Sahar Amiri[2]

[1] Department of Textile Engineering, Amirkabir University of Technology, Tehran, Iran.

[2]Department of Polymer Engineering, Science and Research Branch, Islamic Azad University, Tehran, Iran.

Article Information

Article history:

Received: 2025-05-31

Accepted: 2025-11-15

***Keywords*:**

zinc oxide, sol–gel synthesis, antibacterial activity, electrospinning, polycaprolactone, nanofibers.

Abstract

Nanofibers have attracted increasing attention in biomedical applications owing to their high surface area, porosity, and biocompatibility, which allow them to mimic the extracellular matrix and promote cell adhesion and regeneration. In this study, zinc oxide (ZnO) nanoparticles were synthesized via the sol–gel method using zinc acetate dihydrate as a precursor and were characterized by FTIR, FESEM, and EDAX analyses. The synthesized nanoparticles exhibited an average size of 30–40 nm with uniform dispersion. These nanoparticles, along with commercial ZnO, were incorporated into polycaprolactone (PCL) nanofibers fabricated by electrospinning. The resulting nanofibers displayed diameters in the range of 250–800 nm, depending on the nanoparticle content and electrospinning conditions. Antibacterial activity was evaluated using inhibition zone assays against Escherichia coli (Gram-negative) and Staphylococcus aureus (Gram-positive). PCL nanofibers containing sol–gel derived ZnO showed superior antibacterial efficiency, with inhibition zones up to 42 mm against S. aureus and 28 mm against E. coli, compared with nanofibers containing commercial ZnO. The enhanced activity is attributed to the smaller size, higher surface reactivity, and homogeneous distribution of sol–gel ZnO nanoparticles. These findings highlight the potential of sol–gel ZnO/PCL nanofibers as advanced antibacterial scaffolds for biomedical applications.

1 INTRODUCTION

Over the last few decades, polymer nanofibers have gained significant attention in biomedical engineering, particularly for the development of functional three-dimensional scaffolds with tailored properties such as antibacterial activity [1,2]. Due to their high surface area, porosity, and small pore size, nanofibers provide a favorable microenvironment for cell adhesion and proliferation, making them suitable for a broad range of applications, including wound healing, tissue regeneration, drug delivery, and protective clothing [3–6]. In recent years, electrospun nanofibers have also been investigated for their potential in advanced wound dressings, where their similarity to the extracellular matrix can promote cell migration and tissue repair [7,8].

Among different fabrication techniques, electrospinning has emerged as the most widely used method for producing nanofibers with controllable diameters ranging from the nanometer to micrometer scale [9-11]. In this process, a high-voltage electric field generates fine polymer jets from solution or melt, leading to the deposition of continuous fibers. Importantly, electrospinning allows the incorporation of bioactive agents such as nanoparticles, antibiotics, or natural extracts into the polymer matrix, enabling the production of multifunctional nanofibers with specific biomedical properties [12-14].

Polycaprolactone (PCL) is a biodegradable polyester that is widely used in biomedical applications due to its low cost, biocompatibility, non-toxicity, and compatibility with a variety of inorganic and organic additives [15,16]. Recent studies have shown that PCL-based nanofibers incorporated with nanoparticles such as silver, titanium dioxide, and zinc oxide (ZnO) demonstrate enhanced antibacterial and wound-healing properties [17–20]. Reviews also highlight the versatility of PCL nanofibers as scaffolds for tissue engineering and regenerative medicine [21].

Among the various inorganic agents, ZnO nanoparticles are particularly attractive because of their strong antibacterial activity, low toxicity to mammalian cells, and ability to generate reactive oxygen species that disrupt bacterial membranes [22–23]. Furthermore, ZnO has been reported to enhance fibroblast proliferation and angiogenesis, making it highly relevant for wound healing applications [24,25].

For instance, ZnO-based nanofiber dressings have been reported to boost fibroblast activity while effectively

* Corresponding Author: Hajirb@aut.ac.ir

inhibiting *E. coli* and *S. aureus* growth [26]. However, the antibacterial efficiency of ZnO is highly dependent on particle size, distribution, and synthesis method [27]. Commercial ZnO is widely available, but it often suffers from large particle size and aggregation. Alternatively, sol–gel synthesis offers a simple and cost-effective route to produce uniformly distributed ZnO nanoparticles with nanoscale dimensions [28-29].

Several reports have demonstrated the incorporation of ZnO nanoparticles into PCL nanofibers for biomedical applications [30-32]. Nevertheless, most existing studies rely on commercial ZnO powders, and limited research has compared them with sol–gel-derived ZnO in terms of fiber morphology, antibacterial efficiency, and structural properties.

In the present work, ZnO nanoparticles were synthesized via the sol–gel method and characterized by Fourier-transform infrared spectroscopy (FTIR), field emission scanning electron microscopy (FESEM), and energy-dispersive X-ray spectroscopy (EDAX). Both sol–gel-derived and commercial ZnO nanoparticles were incorporated into electrospun PCL nanofibers, and the resulting structures were characterized for morphology, chemical bonding, and antibacterial performance against *Escherichia coli* (Gram-negative) and *Staphylococcus aureus* (Gram-positive). The novelty of this study lies in the direct comparison of sol–gel-synthesized and commercial ZnO within the same PCL nanofiber matrix, highlighting how particle size and distribution influence antibacterial performance. The findings aim to provide insights into optimizing ZnO/PCL nanofibers as advanced antibacterial scaffolds for biomedical applications.

2 Experimental

2-1 Material

Poly(ε-caprolactone) (PCL, Mw = 60,000–80,000 g/mol) was purchased from Sigma-Aldrich. Zinc acetate dihydrate (≥98%), ethanol (≥98%), isopropyl alcohol (≥98%), dimethyl sulfoxide (DMSO, ≥98%), dichloromethane (DCM, ≥98%), and monoethanolamine (MEA, 99.8%) were obtained from Merck and used as received.

2-2 Synthesis of ZnO nanoparticles

ZnO nanoparticles were synthesized via the sol–gel method using zinc acetate dihydrate as a precursor. Briefly, zinc acetate dihydrate was dissolved in anhydrous isopropyl alcohol and stirred on a magnetic stirrer for 30 min. MEA, serving as a stabilizer, was added dropwise until a transparent solution was obtained. The mixture was further stirred at 60 °C for 2 h and then aged at room temperature for 24 h to form a clear and homogeneous sol [16,17]. The sol was subsequently dried and calcined at 400 °C for 2 h to remove organic residues and obtain crystalline ZnO nanoparticles.

2-3 Electrospinning of PCL/ZnO nanofibers

Electrospinning solutions were prepared by dissolving PCL (25% w/v) in a DMSO/DCM mixture (35/65 v/v). ZnO nanoparticles (5 or 10% w/w relative to PCL) were dispersed ultrasonically into the polymer solution to ensure homogeneity. The resulting suspension was loaded into a 5 mL glass syringe fitted with a 30 G stainless steel needle. Electrospinning was performed at an applied voltage of 15–20 kV, a feed rate of 1 mL/h, and a collector rotation speed of 2000 rpm. The distance between the needle tip and the aluminum foil–covered collector was maintained at 18 cm. All electrospinning experiments were conducted in a controlled environment (23–25 °C, 18% relative humidity) [18–20].

2-4 Characterization

Fourier-transform infrared spectroscopy (FTIR, Equinox 55 spectrometer, Bruker, Germany) was performed in the wavenumber range of 400–4000 cm^{-1} to identify functional groups and confirm the interaction of ZnO nanoparticles with the PCL matrix. The absorption bands were indexed according to standard references to facilitate interpretation. The morphology and fiber diameter of the electrospun nanofibers were examined by scanning electron microscopy (SEM, Philips XL30, Poland) operated at an accelerating voltage of 15 kV. High-resolution field emission scanning electron microscopy (FESEM, Tescan Mira3, Czech Republic) was additionally employed to observe the detailed surface morphology of ZnO nanoparticles and their distribution in the nanofiber matrix. Fiber diameters were measured from SEM micrographs using ImageJ software, and at least 100 fibers per sample were analyzed to obtain average values and distribution histograms. Elemental composition and distribution of Zn and O within the nanofibers were determined by energy-dispersive X-ray spectroscopy (EDAX, INCA, Oxford Instruments, UK). Both qualitative mapping and quantitative analysis were performed to determine the weight and atomic percentage of the elements present.

The antibacterial activity of the PCL/ZnO nanofibers was evaluated against Escherichia coli (ATCC 25922, Gram-negative) and Staphylococcus aureus (ATCC 25923, Gram-positive) using the AATCC 100-2004 test method. Briefly, bacterial suspensions were prepared by inoculating several colonies from each strain into tryptic soy broth (TSB) and incubating overnight at 37 °C. The cultures were adjusted to a turbidity of 1.0 on the McFarland scale (~1×10^7 CFU/mL) and subsequently diluted (1:1,000 or 1:10,000) in fresh TSB to achieve the working inoculum.

Sterilized circular nanofiber samples (8 mm diameter) were incubated with 1 mL of bacterial suspension at 37 °C for 24 h under aerobic conditions. After incubation, 100 µL of the bacterial suspension was transferred to Petri dishes, followed by the addition of molten tryptic soy agar (TSA, 45 °C). Plates were mixed, solidified, and incubated at 37 °C for 24 h. Colony-forming units (CFU) were counted to quantify bacterial survival.

The antibacterial efficacy was expressed by measuring both (i) the reduction in viable CFU compared to control samples and (ii) the diameter of the inhibition halo surrounding the nanofiber disks. Values below 8 mm were considered inactive against microorganisms. Zones of inhibition were recorded for each sample and averaged from triplicate measurements.

3 Results and discussions

3-1 FTIR analysis of ZnO nanoparticles

The FTIR spectrum of ZnO nanoparticles synthesized via the sol–gel method is shown in Figure 1. The characteristic absorption bands in the fingerprint region below 1000 cm^{-1} are attributed to metal–oxygen vibrations. In particular, the strong peaks in the range of 500–600 cm^{-1} correspond to the Zn–O stretching vibrations, confirming the formation of ZnO. A band at ~1634 cm^{-1} can be assigned to O–H bending vibrations of adsorbed water molecules, while a broad absorption band between 3400–3600 cm^{-1} corresponds to the stretching mode of hydroxyl groups on the nanoparticle surface. Peaks near 2950 cm^{-1} are related to C–H stretching vibrations, and minor peaks associated with carboxylate and hydroxyl groups likely originate from residual organic precursors used in the sol–gel process [14–17].

It should be noted that FTIR analysis provides qualitative confirmation of Zn–O bonding but is not sufficient to confirm nanoparticle crystallinity. Previous studies [19,20] have emphasized that X-ray diffraction (XRD) is the most reliable method for verifying phase purity and crystal structure of ZnO. Therefore, future work should include XRD characterization to complement FTIR findings and exclude the presence of residual amorphous phases.

The sol–gel-derived ZnO nanoparticles exhibited an average size of 30–40 nm (from FESEM analysis, Section 3.2), which is significantly smaller and more homogeneously distributed compared to commercial ZnO powders, consistent with earlier reports [21,22]. The smaller size and higher surface reactivity of sol–gel ZnO nanoparticles are expected to enhance their antibacterial performance.

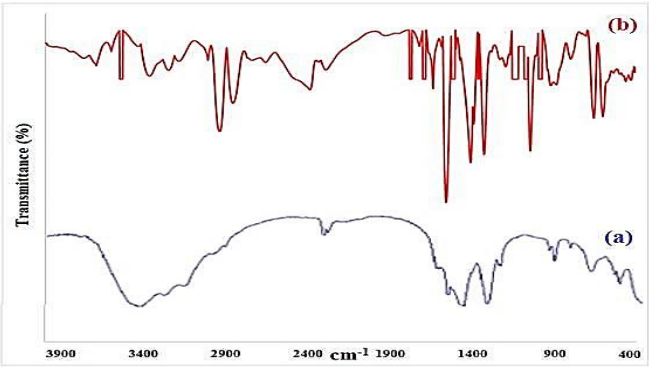

Figure 1 FTIR spectrum of (a) commercial ZnO and (b) ZnO nanoparticles synthesized via the sol-gel method

3-2 Morphological analysis of ZnO nanoparticles

Figure 2 presents the morphology and microstructure of ZnO nanoparticles obtained by the sol-gel method compared to commercial ZnO nanoparticles. The results indicate that sol-gel synthesized nanoparticles are smaller than commercial ones, with particle sizes ranging from 20–30 nm. Energy-dispersive X-ray spectroscopy (EDX) confirmed that the distribution of sol-gel nanoparticles is more uniform. Field-emission scanning electron microscopy (FESEM) also demonstrated a homogeneous dispersion of nanoparticles within the hybrid coatings, without noticeable aggregation [15–18].

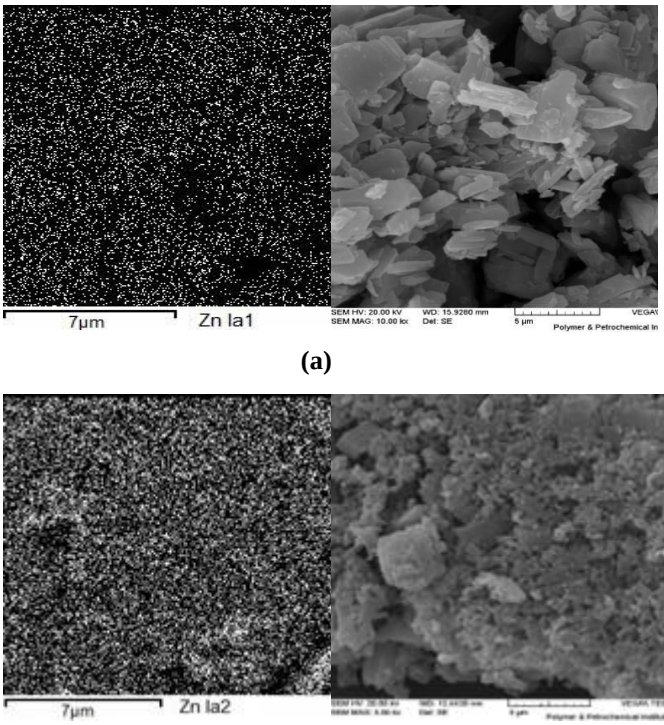

Figure 2 Morphological analysis of ZnO nanoparticles: (a) SEM image of commercial ZnO, (b) SEM image of ZnO synthesized via sol-gel (10% w/w)

3-3 Electrospinning of PCL nanofibers containing nanoparticles

After characterizing the commercial ZnO nanoparticles and those synthesized via the sol-gel method, these nanoparticles were incorporated into PCL nanofibers using the optimized electrospinning conditions. To obtain continuous PCL nanofibers with diameters ranging from approximately 250 nm to 1 µm, several electrospinning parameters—including applied voltage (15, 18, 20Kv), distance between the needle tip and the collector (10, 15, 18 cm), and feed rate (0/5, 1, 1/5 ml/h)—must be optimized [18–20]. In this study, three different values for each parameter were evaluated while maintaining a constant PCL concentration with commercial ZnO nanoparticles.

Fig.3 shows the SEM images of PCL nanofibers obtained under different experimental conditions. The results indicate that continuous fibers with the minimum average diameter were achieved at a feed rate of 1 mL/h, an applied voltage of 20 kV, and a needle-to-collector distance of 18 cm. All subsequent electrospinning experiments were performed under these optimized conditions. Image analysis software (e.g., ImageJ) can be used to determine the fiber diameter distribution and average fiber size for quantitative assessment.

Voltage	feed rate (ml/h)	Distance		
		d=10cm	d=15cm	d=18cm
V=15 kV	(0.5)			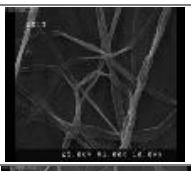
	(1)	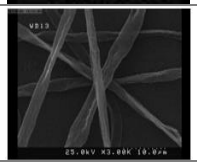	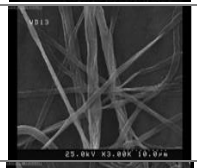	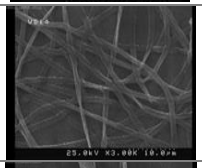
	(1.5)	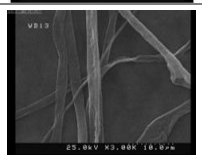	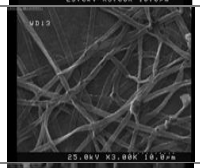	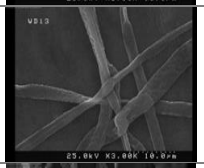
V=18 kV	(0.5)	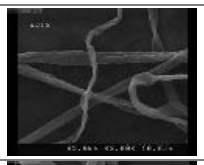	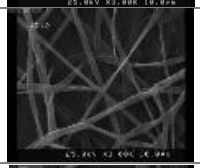	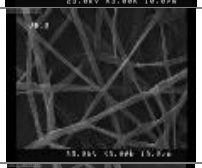
	(1)	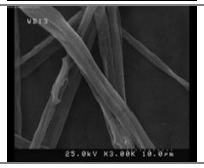	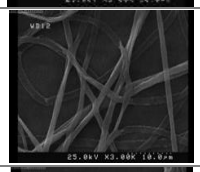	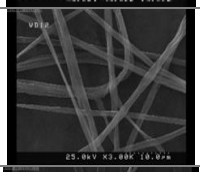
	(1.5)	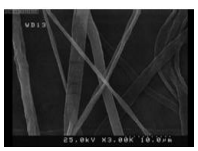	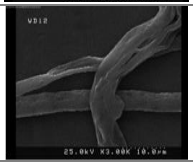	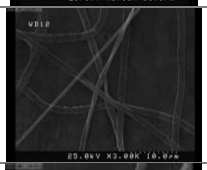
V=20 kV	(0.5)	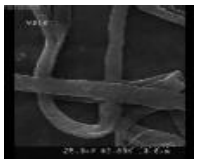	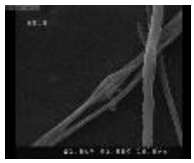	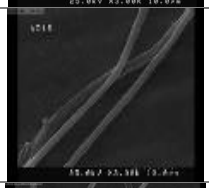
	(1)	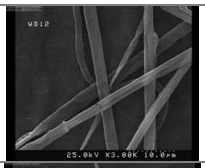	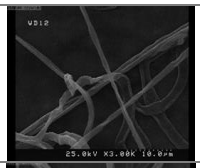	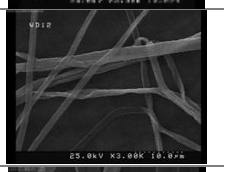
	(1.5)	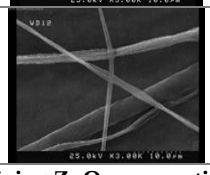	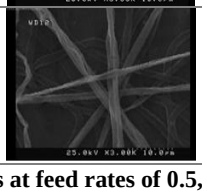	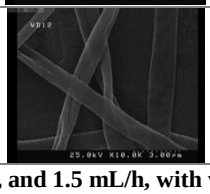

Figure 3 SEM images of PCL nanofibers containing ZnO nanoparticles at feed rates of 0.5, 1, and 1.5 mL/h, with varying applied voltages and needle-to-collector distances

3-4 FTIR analysis of PCL-based nanofibers

Fig.4 presents the FTIR spectra of the PCL-based nanofibers. The characteristic peaks of PCL are observed at: 2865 and 2949 cm^{-1}, corresponding to the asymmetric and symmetric stretching vibrations of the $–CH_2–$ groups, 1727 cm^{-1} for the C=O stretching vibration, 1293 cm^{-1} for C–O and C–C stretching vibrations, 1240 cm^{-1} for the asymmetric C–O–C stretching vibration.

The characteristic ZnO peaks are observed in the range of 550–600 cm^{-1}. Additional peaks at 1643 cm^{-1} and 620 cm^{-1} correspond to stretching and deformation vibrations of Zn–O nanoparticles embedded within the PCL nanofibers [15–17].

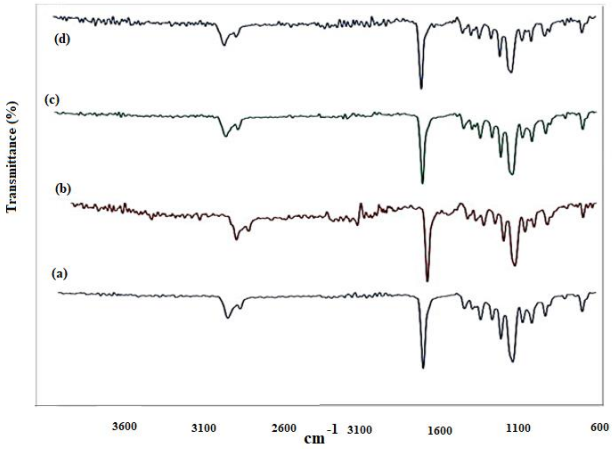

Figure 4 FTIR spectra of (a) pure PCL nanofibers, (b) PCL nanofibers loaded with commercial ZnO, (c) PCL nanofibers loaded with sol-gel ZnO (5% w/w), and (d) PCL nanofibers loaded with sol-gel ZnO (10% w/w)

3-5 Morphology analysis of PCL-based nanofibers

Figure 5 shows the SEM images of pure PCL nanofibers and PCL nanofibers containing ZnO nanoparticles, illustrating the effect of nanoparticle incorporation on fiber morphology.

The addition of ZnO nanoparticles—both commercial and sol-gel synthesized—modifies the surface and structure of the PCL nanofibers. Specifically, the incorporation of commercial ZnO increases the average fiber diameter, which can be attributed to the higher solution viscosity and reduced electrical conductivity during electrospinning [18–20]. In contrast, PCL nanofibers containing sol-gel ZnO nanoparticles exhibit more uniform fibers with smaller diameters, consistent with the smaller size and better dispersion of sol-gel ZnO. Quantitative analysis of fiber diameter distribution using image analysis software (e.g., ImageJ) is recommended to fully characterize these differences.

Agglomeration of ZnO nanoparticles in PCL nanofibers leads to rougher fiber surfaces. The incorporation of 5% w/w sol-gel ZnO nanoparticles decreases the average fiber diameter but increases surface roughness, whereas 10% w/w sol-gel ZnO nanoparticles result in smoother fiber surfaces. This smoothing effect at higher ZnO content is likely due to a decrease in solution viscosity, which facilitates fiber formation and reduces fiber diameter.

Fig.6 presents the EDX spectrum of ZnO nanoparticles, confirming zinc and oxygen as the primary elemental components [21–23]. Fig.6 illustrates the EDX mapping of PCL/ZnO nanofibers, revealing a homogeneous distribution of Zn and O throughout the fibers, which indicates uniform nanoparticle dispersion. For a more detailed assessment of elemental composition, quantitative EDX analysis (including weight and atomic percentages) is recommended.

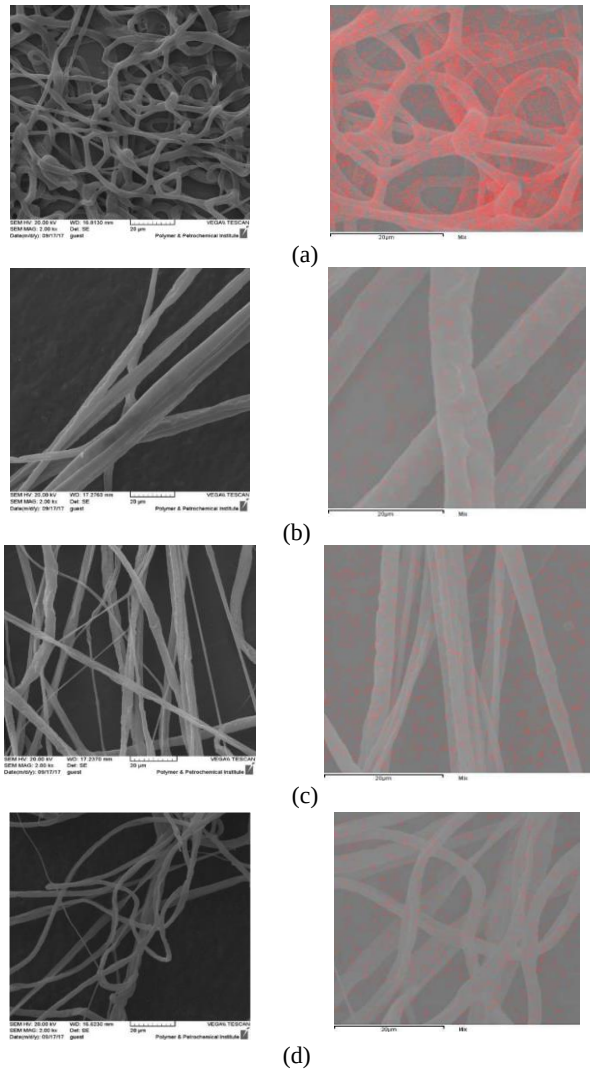

Figure 5 SEM images of (a) pure PCL nanofibers, (b) PCL nanofibers loaded with commercial ZnO nanoparticles, (c) PCL nanofibers loaded with 5% w/w sol-gel ZnO nanoparticles and (d) PCL nanofibers loaded with 10% w/w sol-gel ZnO nanoparticles

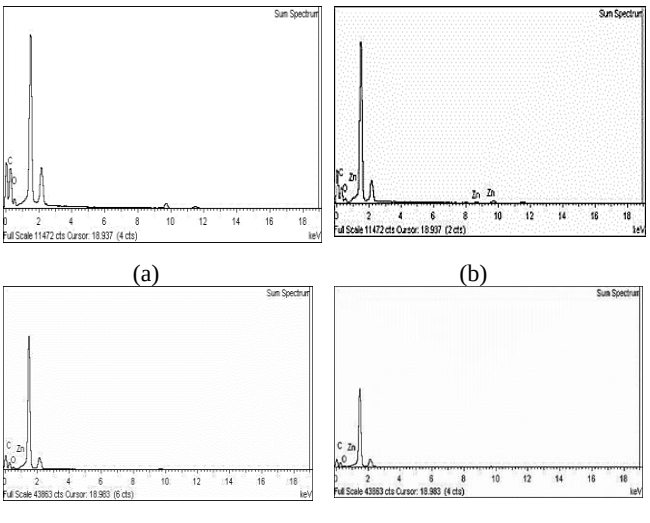

Figure 6 EDX spectra of (a) pure PCL nanofibers, (b) PCL nanofibers loaded with commercial ZnO, (c) PCL nanofibers loaded with sol-gel ZnO (5% w/w), and (d) PCL nanofibers loaded with sol-gel ZnO (10% w/w).Anti-bacterial activities of the PCL/ZnO nanofibers

3-6 Antibacterial Activities of PCL/ZnO Nanofibers

The antibacterial activity of the fabricated nanofibers was evaluated against representative Gram-negative and Gram-positive bacteria using the disk diffusion method. Escherichia coli (E. coli) and Staphylococcus aureus (S. aureus) were chosen as model organisms (Fig.7, Table. 1). Zones of inhibition, measured around the disks including the disk diameter, indicate microbial sensitivity to the nanofibers. Values below 8 mm were considered inactive, while negligible zones indicate resistance.

Pure PCL nanofibers showed no antibacterial effect against either E. coli or S. aureus. PCL nanofibers containing commercial ZnO exhibited antibacterial activity against E. coli but not against S. aureus. This difference is likely due to the thick peptidoglycan layer of S. aureus, which forms clustered, spherical colonies that limit nanoparticle diffusion and reduce antibacterial effectiveness.

In contrast, PCL nanofibers containing sol-gel ZnO nanoparticles inhibited the growth of both E. coli and S. aureus. The enhanced activity is attributed to better nanoparticle dispersion on the nanofiber surface. Increasing the ZnO content from 5% to 10% w/w further enhanced antibacterial activity, likely due to a higher number of nanoparticles, increased surface area, and greater surface reactivity. These factors facilitate bacterial cell wall damage, increased membrane permeability, and enhanced uptake of zinc ions, leading to effective inhibition of cell growth [24–26].

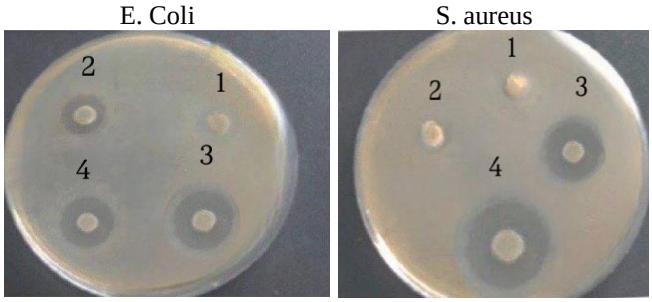

Figure 7 Representative photographs of antibacterial halo tests showing the inhibition of E. coli and S. aureus growth on agar medium: (1) pure PCL nanofibers, (2) PCL nanofibers loaded with commercial ZnO, (3) PCL nanofibers loaded with sol-gel ZnO (5% w/w), and (4) PCL nanofibers loaded with sol-gel ZnO (10% w/w)

Table 1 Diameter of inhibition zone of PCL nanofibers containing ZnO nanoparticles

		Diameter of inhibition zone	
No.	**Sample**	**E.Coli (1.5×10^7)**	**S.aureus (1.5×10^7)**
1	PCL	No	No
2	PCL/ZnO (commercial nanoparticles)	17 mm	No
3	PCL/ZnO (from sol-gel, 5%w/w)	23 mm	35 mm
4	PCL/ZnO (from sol-gel, 10%w/w)	28 mm	42 mm

4 Conclusion

ZnO nanoparticles were successfully synthesized via the sol-gel method and characterized using FTIR, SEM, FESEM, and EDX techniques. FTIR analysis confirmed the formation of ZnO nanoparticles, while SEM and FESEM revealed their nanoscale size and uniform distribution. EDX further demonstrated the elemental composition and homogeneity of the nanoparticles.

Both sol-gel synthesized and commercial ZnO nanoparticles were incorporated into PCL nanofibers, which were subsequently characterized by FTIR, SEM, and EDX. SEM analysis showed that the incorporation of commercial ZnO increased the solution viscosity and resulted in larger nanofiber diameters, likely due to nanoparticle agglomeration. In contrast, sol-gel ZnO nanoparticles decreased the solution viscosity, producing smaller-diameter fibers with rougher surfaces, attributed to better dispersion and interaction with the polymer matrix.

The inclusion of sol-gel ZnO nanoparticles significantly enhanced the antibacterial activity of the PCL nanofibers against both E. coli and S. aureus. This improvement is related to the higher surface area and enhanced surface reactivity of sol-gel ZnO nanoparticles, which facilitate bacterial cell wall disruption, increase membrane permeability, and promote the release of zinc ions. Compared to PCL nanofibers containing commercial ZnO, nanofibers with sol-gel ZnO exhibited superior antimicrobial performance, highlighting the potential of sol-gel ZnO for biomedical and antimicrobial applications.

This study demonstrates the novelty of using sol-gel ZnO nanoparticles to produce well-dispersed, antimicrobial PCL nanofibers, providing both quantitative (fiber diameter, particle size) and qualitative (morphology, antibacterial activity) evidence of their enhanced properties.

REFERENCES

[1] A. Gholipour-Kanani, S.H. Bahrami, S. Rabbani, Effect of novel blend nanofibrous scaffolds on diabetic wounds healing, *IET Nanobiotechnology*, 2015; 10(1): 1–7.

[2] Afsaneh Valipouri, Seyed Abdolkarim Hosseini, Fabrication of Biodegradable PCL Particles as well as PA66 Nanofibers via Air-Sealed Centrifuge Electrospinning (ASCES),*Journal of Textiles and Polymers*,2016; 4(1):15–19.

[3] Jaworek A, Krupa A, Lackowski M, Sobczyk AT, Czech T, Ramakrishna S, Sundarrajan S, Pliszka D. Electrospinning and electrospraying techniques for nanocomposite non-woven fabric production. *Fibres & Textiles in Eastern Europe*, 2009; 17(4): 77–81.

[4] Adeleh Gholipour-Kanani, Pedram Daneshi, A Review on Centrifugal and Electro-Centrifugal Spinning as New Methods of Nanofibers Fabrication, *Journal of Nanostructure Chemistry*, 2022; 10(1): 41–55.

[5] A. Hivechi, S.H. Bahrami, R.A. Siegel, P.B. Milan, M. Amoupour, In vitro and in vivo studies of biaxially electrospun poly(caprolactone)/gelatin nanofibers reinforced with cellulose nanocrystals for wound healing applications, *Cellulose*, 2020; 27: 5179–5196.

[6] A. Gholipour-Kanani, S.H. Bahrami, A. Samadi-Kochaksaraie, H. Ahmadi-Tafti, S. Rabbani, A. Kororian, E. Erfani, Effect of tissue-engineered chitosan-poly(vinyl alcohol) nanofibrous scaffolds on healing of burn wounds of rat skin, *IET Nanobiotechnology*, 2012; 6(4): 129–135.

[7] Faghani A, Hashemi H, Mirzaei M. Emerging nanomaterials for novel wound dressings. *Heliyon*, 2024; 10(3): e26009. https://doi.org/10.1016/j.heliyon.2024.e26009

[8] Palani S, Perumal S, Ramesh B. Electrospun nanofibers synthesized from polymers loaded with nanoparticles on wound healing: A review. *Journal of Nanobiotechnology*, 2024; 22: 91. https://doi.org/10.1186/s12951-024-02491-8

[9]Hosnie Baheri, Seyed Hajir Bahrami, Chitosan/Nanosilver Nanofiber Composites with Enhanced Morphology and Microbiological Properties, *Journal of Textiles and Polymers*, 2015; 3(2): 64–70.

[10] Malihe Ghazalian, Shahnoosh Afshar, Amir Rostami, Shiva Rashedi, Seyed Hajir Bahrami, Fabrication and characterization of chitosan-polycaprolactone core-shell nanofibers containing tetracycline hydrochloride, *Colloids and Surfaces A: Physicochemical and Engineering Aspects*, 2022; 636: 128163.

[11]Krucińska I, Komisarczyk A, Chrzanowski M, Paluch D. Producing wound dressing materials from chitin derivatives by forming nonwovens directly from polymer solution, *Fibres & Textiles in Eastern Europe*, 2007; 15(5-6): 73–76.

[12] Lee KH, Kim HY, Khil MS, Ra YM, Lee DR. Characterization of nano-structured poly(ε-caprolactone) nonwoven mats via electrospinning, *Polymer*, 2003; 44: 1287–1294.

[13] Wang ZL. Zinc Oxide Nanostructures: Growth, properties and applications, *Journal of Physics: Condensed Matter*, 2004; 16: 829–858.

[14] Masoumeh Valizadeh, Seyyed Abdolkarim Hosseini Ravandi, Seerma Ramakrishna, Recent advances in electrospinning of some selected biopolymers, *Journal of Textiles and Polymers*, 2013; 1(2): 70–78.

[15] Farnaz-sadat Fattahi, Akbar Khoddami, Ozan Avinc, Poly(lactic acid) (PLA) Nanofibers for Bone Tissue Engineering, *Journal of Textiles and Polymers*, 2019; 7(2): 47–64.

[16] Kaleji B, Mousaei M, Halakouie H, Ahmadi A. Sol-gel synthesis of ZnO nanoparticles and ZnO-TiO_2-SiO_2 nanocomposites and their photocatalyst investigation in methylene blue degradation, *Journal of Nanostructures*, 2015; 5: 219–225.

[17] Tian J, Chen L, Dai J, Wang X, Yin Y, Wu P. Preparation and characterization of TiO_2, ZnO, and TiO_2/ZnO nanofilms via sol–gel process, *Ceramics International*, 2009; 35: 2261–2270.

[18] Rahimi A, Amiri S. Sol–gel technology and various hybrid nanocomposite coatings applications, *Iranian Polymer Journal*, 2016; 25(6): 559–570.

[19] Zare Estekhraji SA, Amiri S. Sol–gel preparation and characterization of antibacterial and self-cleaning hybrid nanocomposite coatings, *Journal of Coatings Technology and Research*, 2017; 14(6): 1335–1343.

[20] Zare Estekhraji SA, Amiri S. Synthesis and characterization of anti-fungus, anti-corrosion and self-cleaning hybrid nanocomposite coatings based on sol–gel process, *Journal of Inorganic and Organometallic Polymers and Materials*, 2017; 27(4): 883–891.

[21] Robles E, Álvarez C, Rodriguez A. Advances in Electrospun Poly(ε-caprolactone)-based scaffold fabrication and applications in tissue engineering, *Polymers*, 2024; 16(20): 2853. https://doi.org/10.3390/polym16202853

[22] Koushki P, Bahrami SH, Ranjbar-Mohammadi M. Coaxial nanofibers from poly(caprolactone)/poly(vinyl alcohol)/Thyme and their antibacterial properties, *Journal of Industrial Textiles*, 2016. https://doi.org/10.1177/1528083716674906

[23] Ranjbar-Mohammadi M, Bahrami SH. Development of nanofibrous scaffolds containing gum tragacanth/poly(ε-caprolactone) for application as skin scaffolds, *Materials Science and Engineering: C*, 2015; 48: 71–79.

[24] Xiao J, Li H, Zhang L. Zinc oxide nanoparticles for skin wound healing: mechanisms and biomedical applications, *Materials Today Advances*, 2025; 21: 100642. https://doi.org/10.1016/j.mtadv.2025.100642

[25] Hassan S, Bakhshi PK, Chatterjee S. Investigation of angiogenesis and wound healing processes via ZnO nanorods, *International Journal of Nanomedicine*, 2021; 16: 8151–8164. https://doi.org/10.2147/IJN.S326384

[26] Mahmoudnezhad A, Haghjooy Javanmard S, Akbarzadeh A. Core–shell nanofiber dressings with zinc oxide nanoparticles and cell-free fat extract: boosting fibroblast activity and antibacterial efficacy, *Journal of Biological Engineering*, 2025; 19: 32. https://doi.org/10.1186/s13036-025-00511-1

[27] Ranjbar-Mohammadi M, Bahrami SH, Rabbani, Joghataei MT, Moayere F. Antibacterial performance and in vivo diabetic wound healing of curcumin-loaded gum tragacanth/poly(ε-caprolactone) electrospun nanofibers, *Materials Science and Engineering: C*, 2016; 69: 1183–1191.

[28] Augustine R, Malik HN, Singhal DK, Mukherjee A, Malakar D, Kalarikkal N, Thomas S. Electrospun polycaprolactone/ZnO nanocomposite membranes as biomaterials with antibacterial and cell adhesion properties, *Journal of Polymer Research*, 2014; 21(3): 1–17.

[29] Augustine R, Dominic EA, Reju I, Kaimal B, Kalarikkal N, Thomas S. Electrospun polycaprolactone membranes incorporated with ZnO nanoparticles as skin substitutes with enhanced fibroblast proliferation and wound healing, *RSC Advances*, 2014; 4(47): 24777–24785.

[30] Radulescu M, Andronescu E, Cirja A, Holban AM, Mogoanta L, Balseanu TA, Catalin B, Neagu TP, Lascar I, Florea DA, Grumezescu AM, Ciubuca B, Lazar V, Chifiriuc MC, Bolocan A. Antimicrobial coatings based on zinc oxide and orange oil for improved bioactive wound dressings and other applications, *Romanian Journal of Morphology and Embryology*, 2016; 57: 107–114.

[31] Prasad D, Girija CR, Jagannatha Reddy A, Nagabhushana H, Nagabhushana BM, Venkatesha TV, Arun Kumar ST. A study on the antibacterial activity of ZnO nanoparticles prepared by combustion method against *E. coli*, *Journal of Engineering Research and Applications*, 2014; 4: 84–89.

[32] Salem W, Leitner DR, Zingl FG, Schratter G, Prassl R, Goessler W, Reidl J, Schild S. Antibacterial activity of silver and zinc nanoparticles against *Vibrio cholerae* and enterotoxic *Escherichia coli*, *International Journal of Medical Microbiology*, 2015; 305(1): 85–95.